

RESEARCH ARTICLE

Theranostic-guided corneal cross-linking: Preclinical evidence on a new treatment paradigm for keratoconus

Giuseppe Lombardo^{1,2}  | Giuseppe Massimo Bernava¹  | Sebastiano Serrao³ | Marco Lombardo^{2,3} 

¹CNR-IPCF, Istituto per i Processi Chimico-Fisici, Viale F, Messina, Italy

²Vision Engineering Italy srl, Rome, Italy

³Studio Italiano di Oftalmologia, Rome, Italy

Correspondence

Giuseppe Lombardo, MEng, PhD, CNR-IPCF, Istituto per i Processi Chimico-Fisici, Viale F. Stagno D'Alcontres 37, 98158, Messina, Italy.

Email: giuseppe.lombardo@cnr.it

Marco Lombardo, MD, PhD, Vision Engineering Italy srl, Via Livenza 3, 00198 Rome, Italy.

Email: mlombardo@visioeng.it

Funding information

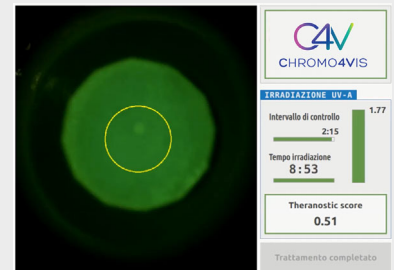
Lazio Innova, Grant/Award Number: A0114-2017-13715

Abstract

Theranostics is an emerging therapeutic paradigm of personalized medicine; the term refers to the simultaneous integration of therapy and diagnostics. In this work, theranostic-guided corneal cross-linking was performed on 10 human sclero-corneal tissues. The samples were soaked with 0.22% riboflavin formulation and underwent 9 minutes UV-A irradiance at 10 mW/cm² using theranostic device, which provided both a measure of corneal riboflavin concentration and a *theranostic score* estimating treatment efficacy in real time. A three-element viscoelastic model was developed to fit the deformation response of the cornea to air-puff excitation of dynamic tonometry and to calculate the mean corneal stiffness parameter before and after treatment. Significant correlation was found between the *theranostic score* and the increase in mean corneal stiffness ($R = 0.80$; $P < .001$). Accuracy and precision of the *theranostic score* in predicting the induced corneal tissue stiffening were both 90%. The riboflavin concentration prior to starting the UV-A photo-therapy phase was the most important variable to allow corneal cross-linking to be effective. Theranostic UV-A light mediated imaging and therapy enables the operator to adopt a precise approach for achieving highly predictable biomechanical strengthening on individual corneas.

KEYWORDS

corneal cross-linking, keratoconus, riboflavin, theranostics



Abbreviations: CXL, corneal cross-linking; Thera-CXL, theranostic guided corneal cross-linking.

Giuseppe Lombardo and Marco Lombardo contributed equally to this work.

This is an open access article under the terms of the [Creative Commons Attribution-NonCommercial-NoDerivs](https://creativecommons.org/licenses/by-nc-nd/4.0/) License, which permits use and distribution in any medium, provided the original work is properly cited, the use is non-commercial and no modifications or adaptations are made.

© 2022 The Authors. *Journal of Biophotonics* published by Wiley-VCH GmbH.

1 | INTRODUCTION

Riboflavin/UV-A corneal cross-linking (CXL) is a widely established treatment option for patients with keratoconus and corneal ectasia. The procedure has a high-

benefit–risk profile, although treatment efficacy (indicated as flattening of the maximum keratometry value, K_{\max}) is largely variable among studies, with a reported median efficacy of 70% of treated cases and a failure rate ranging from 8% to 33% 1 year after surgery [1–4]. The wide variation in the reported clinical efficacy of CXL has been associated with two main factors, including (a) the lack of standardization of the procedure, including several treatment protocols differing for the presence of corneal epithelium, the type and time of riboflavin dosing, the UV-A irradiation power density and energy dose and (b) the phenotypic diversity of keratoconus, including the intrinsic disease heterogeneity in biology and biomechanics [5, 6].

Understanding the principles of UV-A interaction with the cornea soaked with riboflavin could be fundamental to effective and precise management of keratoconus with CXL [7–10]. The exact molecular mechanism of riboflavin/UV-A corneal cross-linking is still under investigation. It involves the formation of additional intramolecular collagen crosslinking bonds and additional bonds between the collagen molecules and between collagen and proteoglycans core proteins [7, 11, 12]. Riboflavin is a unique photochemical agent because it can act as a photosensitizing agent and the tight-excited molecule itself can also act as an electron donor [13]. In the presence of UV-A light, riboflavin exhibits photosensitizing properties, reacting with a wide range of electron-donating substrates or even in the absence of added electron donor, through mixed Type I and Type II photochemical mechanisms, which can be favored or not by the presence of oxygen [11, 14, 15]. Previous authors have demonstrated that the main mechanism of the corneal cross-linking treatment is the direct interaction between riboflavin triplets and reactive groups of stromal proteins, which leads to the cross-linking of the proteins through radical reactions [7, 16]. This implies that, in ambient environment (ie, 21% partial pressure of oxygen), the amount of riboflavin into the stroma and the role of type I mechanism are predominant for the formation of additional chemical bonds between stromal proteins [7, 16].

In previous studies [17–19], we have demonstrated the reliability of a theranostic UV-A prototype device to assess the photo-kinetics of corneal riboflavin in standard (3 mW/cm² for 30 minutes) and accelerated CXL (10 mW/cm² for 9 minutes) protocols as well as in a transepithelial protocol with iontophoretic delivery of riboflavin. In addition, we have determined that the CXL induced biomechanical strengthening of the corneal tissue, which has been assessed by atomic force microscopy, was significantly correlated with the amount of stromal riboflavin (before UV-A irradiation) and its UV-A light-mediated photo-degradation [17–19].

Theranostics, which is a portmanteau word of *therapy* and *diagnostics*, represents one of the most advanced method of transition from conventional to *personalized* and *precision medicine*. A theranostic medical device is able to measure in real time the concentration of a therapeutic molecule into the targeted tissue area and simultaneously to treat it, with real time assessment of treatment efficacy [20]. Light activated image-guided drug therapy finds an ideal use in CXL treatment; under UV-A light illumination, the photosensitizing riboflavin molecule responds to the controlled photo-irradiation inducing both imaging and therapy at targeted corneal location. The scope of this study was to assess the performance of a theranostic UV-A medical device in improving corneal tissue biomechanical strength with precision and accuracy in eye bank human donor sclero-corneal tissues.

2 | EXPERIMENTAL SECTION

2.1 | Human donor tissues

Eye bank human donor tissues from different donors were obtained from the Veneto Eye Bank Foundation (Venezia Zelarino, Italy). The samples were shipped to the laboratory in 6% dextran-enriched corneal storage medium and were used for experiment within 10 hours. Inclusion criterion was an endothelial cell density > 1600 cells/mm²; exclusion criteria included history of corneal pathologies, traumas or eye surgery. The study adhered to the tenets of Declaration of Helsinki for the use of human tissues.

A total of 14 sclero-corneal tissues were used for experiments. The mean donor age was 64.3 ± 6.4 years, the mean cadaver time was 10.8 ± 5.5 hours; the mean endothelial cell density was 2000 ± 315 cells/mm² (Axiovert 25, Carl Zeiss Microscopy, Jena, Germany); the average central corneal thickness (CCT) of the tissues with intact epithelium was 608 ± 102 μ m (OCT-HS-100, Canon, Japan).

The sclero-corneal tissues were de-epithelialized immediately before commencing the experiment using an Amoils' brush (Innovative Excimer Solutions Inc., Toronto, Canada). Each tissue was placed in an artificial anterior chamber (AAC, Coronet, Network Medical Products Ltd, North Yorkshire, UK) pressurized with the AAC filled with 0.9% sodium chloride; the AAC was connected, through tubing, to a column manometer in order to maintain intracameral pressure within a physiological ranges during experiment.

Ten sclero-corneal tissues underwent theranostic-guided corneal cross-linking (Thera-CXL), two samples were left untreated and used as negative controls and two samples were immersed in 2.5% glutaraldehyde solution for 5 hours and used as positive controls.



FIGURE 1 Main Thera-CXL treatment steps. A, The device allows the operator to focus onto the cornea to treat with Placido-disc technology; thereafter, the operator acquires the baseline image of the cornea. At preset monitoring time intervals, both during dosing and UV-A photo-therapy phases, the device acquires, processes and calculates the fluorescence emission signal of the cornea illuminated by 3 mW/cm^2 UV-A power density for a few seconds in order to estimate the corneal riboflavin concentration. B, The panel shows the measurement of corneal riboflavin concentration at 10 minutes time interval during dosing phase. C, During UV-A photo-therapy, the devices tracks the photo-degradation of corneal riboflavin and calculates the *theranostic score* providing an estimation of treatment efficacy. The panel shows the measurement of corneal riboflavin concentration and the *theranostic score* a few seconds before UV-A photo-therapy ending.

2.2 | Theranostics technology for corneal cross-linking

Treatment procedure was performed using a theranostic UV-A medical device (C4V CHROMO4VIS sw 2.0, Regensight srl, Italy). The main components of the device includes a UV-A light Led ($365 \pm 10 \text{ nm}$), which emits a controlled power density for theranostic imaging and therapy, a RGB camera, which acquires the images emitted by the cornea when illuminated by UV-A light, and a single board computer, which manages the correct operation of the electro-optical components, processes the camera images and calculates two imaging biomarkers estimating the corneal riboflavin concentration and treatment efficacy in real-time during surgery [17–19].

The operator performs Thera-CXL through the interaction with the device's touchscreen, which displays the cornea to treat. At the beginning of each treatment, the theranostic UV-A medical device acquires and processes the green signal of the RGB camera, which corresponds to the native fluorescence of the cornea illuminated by 3 mW/cm^2 UV-A power density. This value is subtracted from the averaged green RGB image value, which is acquired by the camera at preset time intervals both during the soaking phase and the UV-A photo-therapy phase of Thera-CXL, and is processed to estimate the corneal riboflavin concentration. In addition, during the UV-A photo-therapy phase of Thera-CXL, the device calculates a *theranostic score* estimating treatment efficacy in real time [17–19]. Calculation of the *theranostic score* takes into account the corneal riboflavin dose prior to start UV-A photo-therapy phase and the amount of riboflavin photo-degraded by UV-A light therapy in the cornea under treatment.

2.3 | Theranostic-guided corneal cross-linking

During the soaking phase, a drop of 0.22% riboflavin ophthalmic solution (RitSight, Regensight srl, Italy) was applied every 20 seconds onto the cornea for a total time period ranging between 5 minutes and 15 minutes in order to achieve a variable amount of riboflavin into the cornea prior to UV-A light therapy. Therefore, all corneal tissues underwent 10 mW/cm^2 UV-A irradiance for 9 minutes (5.4 J/cm^2 total UV-A energy) over an irradiation area of 7.00 mm diameter. No riboflavin was applied over the corneal surface during irradiation. Both during the soaking and UV-A light therapy phases, theranostic imaging was performed over a 3.0 mm central area of the cornea at preset time intervals. The main Thera-CXL treatment steps are exemplified in Figure 1.

2.4 | Corneal tissue deformation response

A dynamic tonometry device (Corvis, Oculus Optikgeräte GmbH, Germany) was used to assess the corneal tissue deformation response to an air-puff pulse before and 2-hours after Thera-CXL; negative control tissues underwent testing at baseline time and 2-hours later; positive control tissues underwent testing at baseline time and 5-hours after 2.5% glutaraldehyde solution bath.

The air-puff device is composed of an air compressor emitting a controlled air puff (about 3 mm diameter) as a Scheimpflug image is in focus with the cornea. The release of the air puff is synchronized with an ultrafast Scheimpflug camera that captures 140 corneal images during the air puff event (about 30 ms). The corneal

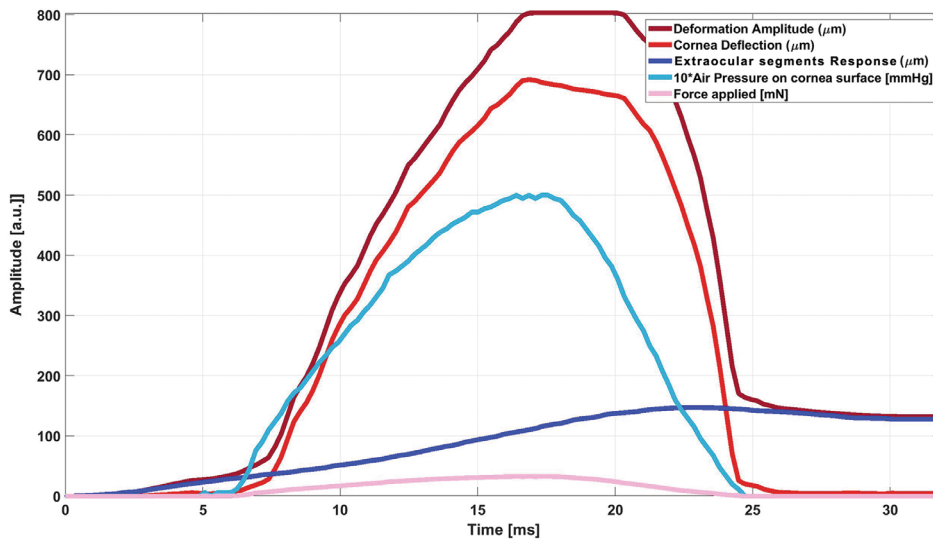


FIGURE 2 Parameters extracted from data processing of image frames acquired during corneal tissue deformation to air excitation by dynamic tonometry device. The blue line represents the force applied by the air pulse on the corneal apex; the red line and the purple line represent the effective corneal deflection and the movement of extraocular tissues in response to air pulse respectively

profile for each image captured during the deformation event was exported from the Corvis software (.avi format; n. 140 frames of 200 x 576 pixels) and processed using custom software written in Matlab (Mathworks Inc., California) [21–23]. The algorithm fitted the anterior and posterior curvature of the corneal tissue with an eight degree polynomial curve and, from corneal deformation data, calculated the following parameters:

- the effective corneal deflection in response to the air pulse;
- the corneal curvature;
- the movement of the extracorneal tissue segments in response to the air pulse;
- the global corneal deformation, which consists of the sum of the corneal deflection, the response of the extra-corneal tissue segments and the corneal curvature;
- the two moments of corneal appplanation and the moment in which the maximum deflection occurs, that is, the cornea assumes a convex curvature;
- the corneal apex point;
- the maximum corneal deflection point;
- the rate of corneal deflection.

Figure 2 shows the main corneal parameters analyzed by dynamic tonometry image frames.

A three-element viscoelastic rheological model was developed to fit the corneal deformation and to calculate the mean corneal stiffness parameter (k_c ; N/m) [24], based upon a modified differential equation, as follows [25, 26]:

$$F_{air-puff} = k_c u_1(t) + k_g u_2(t) + \mu_g \frac{du_2(t)}{dt} \quad (1)$$

The model takes into account both the effective corneal deflection, $u_1(t)$, and the response of the extra-corneal

tissue segments, $u_2(t)$. The sum $u(t) = u_1(t) + u_2(t)$ determines the global deformation of the corneal tissue, $k_c * u_1(t)$ is the force exerted onto the corneal tissue, $k_g * u_2(t) + \mu_g * du_2(t)/dt$ is the force exerted on the extra-corneal tissue, k_g (N/m) represents the extra-corneal tissue stiffness, μ_g (N*s/m) represents the extra-corneal tissue viscosity; k_c (N/m) represents the mean corneal stiffness parameter; it can varies (nonlinear elastic response) as a function of the applied air-puff pressure exerted on the tissue, that is, $k_c = \beta e^{\alpha P_{air-puff}}$, which is the typical behavior for viscoelastic systems [27]. For this reason, the corneal stiffness parameter was calculated as the mean of all k_c at corresponding $P_{air-puff}$, describing accurately the corneal tissue stiffness increase as air pulse pressure varies [21]. Furthermore, the force applied by the air pulse was expressed as $F_{air-puff} = P_{air-puff} * Appl$, where $Appl$ is the appplanation area onto the cornea, which was considered constant and equal to a circle with 2.5 mm diameter [28]. The modified differential equation of the three elements model consisted in determining the mean corneal stiffness parameter, k_c , rather than Young's modulus (E) in order to improve the fit between experimental dynamic tonometry data and the theoretical model (Figure 3) [29]. The model was solved for each sample with a levenberg–marquardt least square minimization algorithm.

2.5 | Data analysis

In this study, data were given as mean \pm standard deviation (SD), and the concentration of riboflavin was expressed as $\mu\text{g}/\text{cm}^3$, where $100 \mu\text{g}/\text{cm}^3 = 0.01\%$. The *theranostic score* is dimensionless value.

A minimum sample of five tissues from the positive group (ie, *theranostic score* predicting increased corneal stiffness correctly) and five tissues from the negative

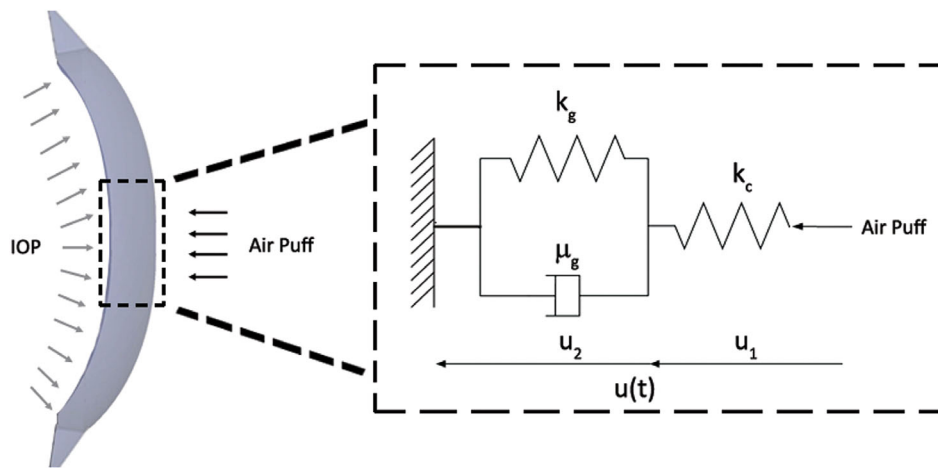


FIGURE 3 Modified viscoelastic rheological model with three elements used for fitting dynamic tonometry testing data. The model describes the contribution of different parameters to the deformation of the sclero-corneal tissue in response to the rapid air pulse excitation. It assumes the cornea as an elastic material (first spring element) and the extra-corneal tissue segments as a viscoelastic material (second spring element and dashpot). The model was able to accurately describe the increase in mean corneal stiffness, $k_{c\text{post}}/k_{c\text{pre}}$, induced by corneal cross-linking either with riboflavin/UV-A light or with 2.5% glutaraldehyde

subgroup achieved 80% power to detect a difference of 0.30 between the area under the ROC curve (AUC) under the null hypothesis of 0.50 and an AUC under the alternative hypothesis of 0.80 using a two-sided z-test at a significance level of 0.05.

The correlation between treatment variables (riboflavin concentration, *theranostic score* and corneal stiffness parameter) was expressed with Pearson correlation coefficient.

In order to assess the prediction ability of the *theranostic score* in assessing CXL outcome, a regression model was developed to correlate it with the induced change in mean corneal stiffness parameter; a second order polynomial regression analysis was performed to correlate the mean corneal stiffness parameter change, Y or $k_{c\text{ post}}/k_{c\text{ pre}}$, with the predictor variable *theranostic score*:

$$Y = b_0 + b_1 * \text{therascore} + b_2 * \text{therascore}^2 \quad (2)$$

where b_0 , b_1 and b_2 are the coefficients of regression.

The accuracy and precision of the model incorporating the *theranostic score* for predicting the increase in corneal stiffness were determined by calculating the proportion of correctly classified samples and the positive predictive value (PPV) respectively.

Statistical analyses were performed using SPSS statistical software (SPSS Inc., ver. 17, IBM), and $P < .05$ was considered as statistically significant.

3 | RESULTS AND DISCUSSION

Theranostic-guided corneal cross-linking consists of two main phases; the first one, during application of

TABLE 1 Corneal riboflavin concentration measured by theranostic UV-A medical device during dosing phase of Thera-CXL

Time (minutes)	Average (\pm SD) concentration ($\mu\text{g}/\text{cm}^3$)
1	32 \pm 14
3	109 \pm 38
5	256 \pm 43
8	286 \pm 83
10	428 \pm 119
12	478 \pm 100
15	525 \pm 105

Note: The results are averaged from a total of 10 human donor corneal tissues undergoing variable total dosing time ranging between 5 minutes ($n = 10$) and 15 minutes ($n = 5$).

riboflavin formulation, including light-mediated measures of the corneal riboflavin concentration providing the operator with a quantitative imaging biomarker of this variable in real time; the latter, during UV-A phototherapy, in which the UV-A light is used both for quantitative imaging and therapy. During the latter treatment phase, the theranostic UV-A medical device provides a *theranostic score*, which is calculated taking into account the corneal riboflavin concentration achieved prior to starting the UV-A photo-therapy phase and the amount of UV-A mediated photo-degraded riboflavin in the individual cornea.

In this laboratory experiment, corneal riboflavin concentration increased with application time ranging from 32 \pm 14 $\mu\text{g}/\text{cm}^3$ at 1 minute to 525 \pm 105 $\mu\text{g}/\text{cm}^3$ at

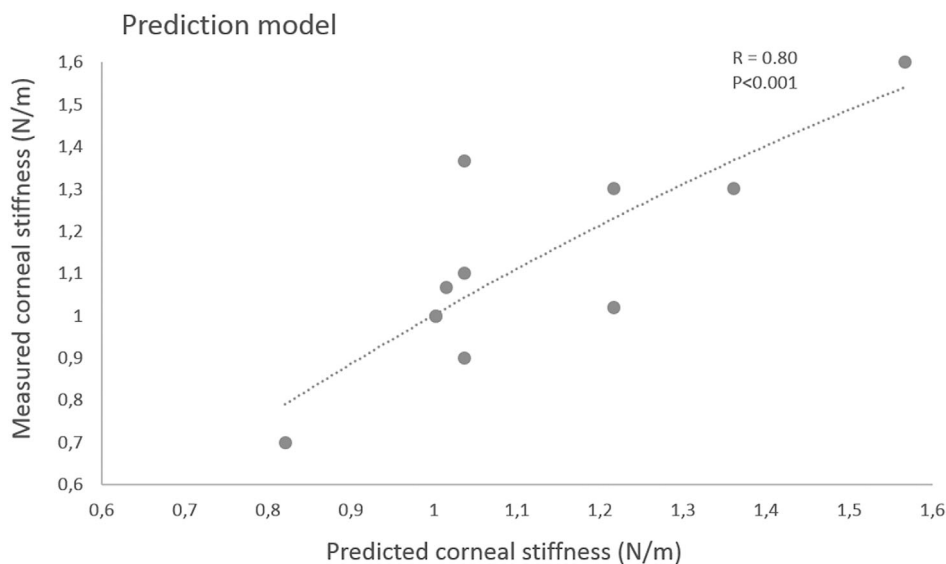


FIGURE 4 Correlation between the tissue biomechanical strengthening, expressed by the mean corneal stiffness parameter k_c (N/m), induced by corneal cross-linking treatment and that predicted by a second order polynomial regression model incorporating the *theranostic score* as predictor. Each symbol represents a human donor corneal tissue treated by CXL ($n = 10$)

15 minutes; table 1 summarizes the average riboflavin corneal concentration measured by the theranostic UV-A device during soaking phase. At the end of UV-A phototherapy phase, the corneal riboflavin concentration averagely decreased by $42 \pm 9\%$ with respect the end of dosing phase and the average *theranostic score* was 1.0 ± 0.3 a.u.. The higher the stromal riboflavin concentration, the greater the *theranostic score* at the end of UV-A photo-therapy phase ($R = 0.71$; $P = .008$). The mean corneal stiffness parameter increased from 36.2 ± 4.7 N/m to 40.9 ± 4.2 N/m. The result of the regression model ($Y = -0.43 + 1.7382x - 0.3066x^2$) was highly statistically significant ($R = 0.80$ and $P < .001$; Figure 4); accuracy and precision of the model were both 90%.

The riboflavin concentration prior to starting the UV-A photo-therapy phase has been confirmed to be the most important variable to allow corneal cross-linking to be effective; under 10 mW/cm^2 UV-A irradiance for 9 minutes with total 5.4 J/cm^2 energy dose, we found a highly significant correlation between the corneal riboflavin dose and the *theranostic score*; the higher the stromal riboflavin concentration, the greater the *theranostic score* ($R = 0.71$; $P = .008$). In order to generate variance among tissues and validate the accuracy of the *theranostic score* in assessing treatment efficacy, the dosing time of riboflavin onto the cornea ranged between 5 and 15 minutes prior to starting the UV-A photo-therapy phase. A second order polynomial regression model incorporating the *theranostic score* as predictor of treatment efficacy had 90% accuracy and 90% precision in predicting the tissue biomechanical strengthening, which was assessed by the mean corneal stiffness parameter, induced by corneal cross-linking. This result highlighted the potential of this imaging biomarker in real time prediction of tissue biomechanical strengthening during CXL in vivo.

In this study, the corneal deformation response under air puff excitation was modeled using a modified three-element spring-dashpot model (Figure 4). The model has already been used in interpreting the corneal material properties in a variety of clinical conditions (including after corneal cross-linking) and the mean corneal stiffness parameter (k_c ; N/m) has been previously validated as a marker to understand changes of corneal strength, resulting to be significantly reduced in corneal diseases in vivo [27, 30]. Corneal stiffness represents the resistance to deformation under load and is a strain dependent value that changes with strain (or corneal deformation). In this study, consistency of the mean corneal stiffness parameter in providing a measure of corneal tissue elasticity was further assessed by investigating the behavior of negative (ie, untreated tissues) and positive (ie, glutaraldehyde treated tissues) controls. Untreated controls did not show any significant change in mean corneal stiffness parameter during experiments (from 34.4 ± 2.9 N/m to 34.9 ± 2.8 N/m); on the other hand, chemical cross-linking with 2.5% glutaraldehyde highly increased the man corneal stiffness parameter from 31.4 ± 2.0 to 93.9 ± 3.0 N/m.

Taking into account the loading magnitude (greater than 45 mmHg) and rate (shorter than 20 ms; see the x-axis in Figure 2), previous authors have shown that the cornea is not able to undergo any viscous deformation during the air-puff event and this explains why pure elastic material model, as done in this study, has been usually selected for biomechanical modeling of the cornea in dynamic tonometry tests [27, 31, 32]. In addition, previous studies have shown that viscosity effects do not substantially contribute to the corneal response during Corvis ST testing [25, 33–35].

Corneal tissue parameters, such as corneal curvature, corneal thickness and intraocular pressure, which could

influence the air-puff device measurements, were accurately monitored in this study. Specifically, intraocular pressure has been identified as the primary variable influencing corneal deformation to air-puff excitation [25, 36–38]. Corneal tissues' parameters were stable during experiments; the CCT of treated tissues ranged from $608 \pm 102 \mu\text{m}$ to $598 \pm 72 \mu\text{m}$ and the corneal curvature from $7.7 \pm 0.3 \text{ mm}$ to $7.6 \pm 0.3 \text{ mm}$ from preoperatively to 2-hours postoperatively; the intracameral pressure values were comparable among preoperatively ($11.1 \pm 3.4 \text{ mmHg}$) and 2-hours postoperatively ($11.3 \pm 2.7 \text{ mmHg}$). No change in any of these parameters was found throughout the experiments, thus eliminating the risk of methodology bias.

Limitations of the study included the lack of anisotropic properties in the biomechanical model and that it did not segregate the sclera contribution to the deformation amplitude; using finite element analysis, authors have hypothesized that the corneal deformation may differ under different ex vivo boundary conditions of fixed versus flexible limbus showing that the sclera could play a role in assessing corneal biomechanics [39]. Despite these limitations, the high accuracy and precision of the prediction model and the results of data on untreated tissues and tissues that underwent chemical cross-linking with glutaraldehyde confirmed the robustness of the method chosen to assess the biomechanical strengthening of the cornea induced by CXL.

The present results were in accordance with previous studies using theranostic UV-A prototype device [17–19]; where the amount of stromal riboflavin prior to UV-A photo-therapy and its UV-A light mediated photodegradation correlated with treatment efficacy when delivering 5.4 J/cm^2 UV-A energy dose. In this study, we used a 0.22% riboflavin ophthalmic solution achieving in 5 minutes ($256 \mu\text{g/cm}^3$) and 10 minutes ($428 \mu\text{g/cm}^3$) average stromal concentration values comparable with 30 minutes soaking with 20% dextran-enriched 0.1% riboflavin ($160 \mu\text{g/cm}^3$) [17, 18] and dextran-free 0.1% riboflavin ($425 \mu\text{g/cm}^3$) [19] respectively. The advantage of using dextran-free ophthalmic solution for corneal soaking is in not inducing any significant change in corneal thickness during treatment, which could be severely thinned by dextran-enriched solutions, which in turn correlated with decreased treatment safety [10, 40, 41]. An ophthalmic solution with high and stable concentration of riboflavin, as used in this study, would be desirable for hastening the soaking phase time duration during CXL, while maintaining a high safety-benefit profile. Adequate corneal soaking with riboflavin has been widely shown to provide a constant concentration of riboflavin up to $350 \mu\text{m}$ stromal depth [8, 42–44], in this view, system confocality would not add any advantage to quantitative imaging during Thera-CXL.

4 | CONCLUSION

Theranostics technology can provide an effective imaging-guided solution for estimating corneal cross-linking clinical efficacy in real time through noninvasive measurement of corneal riboflavin concentration and its UV-A light mediated photo-degradation. In this study, the *theranostic score* imaging biomarker provided accurate prediction of tissue strengthening during corneal cross-linking treatment. Implementing theranostics technology in a UV-A device for corneal cross-linking could be advantageous to minimize the occurrence of treatment failure and to provide personalized patient care. Further studies assessing the performance of Thera-CXL using various UV-A irradiation protocols as well as transepithelial soaking protocols will provide valuable information to assess the overall worth of theranostics technology in improving care to patients with keratoconus.

AUTHOR CONTRIBUTIONS

Giuseppe Lombardo and Marco Lombardo were involved in conceptualization, investigation, writing original draft, project management. Sebastiano Serrao and Giuseppe Massimo Bernava were involved in investigation, data analysis, review and editing original draft.

ACKNOWLEDGMENTS

A part of this work was funded by Lazio Innova POR FESR 2014–2020, grant n. A0114–2017–13715. We are thankful to Davide Camposampiero, Andrea Grassetto and Diego Ponzin (Veneto Eye Bank Foundation, Venezia Zelarino, Italy) for their work in processing eye bank donor tissues for experiments. Open Access Funding provided by Consiglio Nazionale delle Ricerche within the CRUI-CARE Agreement.

CONFLICTS OF INTEREST

- i. Sebastiano Serrao declares no financial or commercial conflict of interest.
- ii. Giuseppe Massimo Bernava declares no financial or commercial conflict of interest.
- iii. Marco Lombardo is co-inventor on an issued patent (IT102016000007349; WO2017130043A1) related to this work.
- iv. Giuseppe Lombardo is co-inventor on an issued patent (IT102016000007349; WO2017130043A1) related to this work.


DATA AVAILABILITY STATEMENT

Research data are not shared.

ORCID

Giuseppe Lombardo  <https://orcid.org/0000-0002-9416-967X>

Giuseppe Massimo Bernava  <https://orcid.org/0000-0001-8024-1338>

Marco Lombardo  <https://orcid.org/0000-0001-8842-7102>

REFERENCES

- [1] S. M. Ng, B. S. Hawkins, I. C. Kuo, *Am. J. Ophthalmol.* **2021**, 229, 274.
- [2] D. F. P. Larkin, K. Chowdhury, J. M. Burr, M. Raynor, M. Edwards, S. J. Tuft, C. Bunce, E. Caverly, C. Doré, KERALINK Trial Study Group, *Ophthalmology* **2021**, 128(11), 1516.
- [3] S. Serrao, G. Lombardo, M. Lombardo, *Int. Ophthalmol.* **2022**, 42(1), 337.
- [4] H. Kobashi, O. Hieda, M. Itoi, K. Kamiya, N. Kato, J. Shimazaki, K. Tsubota, The Keratoconus Study Group Of Japan, *J. Clin. Med.* **2021**, 10(12), 2626.
- [5] A. Gordon-Shaag, M. Millodot, E. Shneur, Y. Liu, *Biomed. Res. Int.* **2015**, 2015, 795738.
- [6] I. M. Y. Cheung, C. N. J. McGhee, T. Sherwin, *Clin. Exp. Optom.* **2013**, 96(2), 188.
- [7] M. Lombardo, G. Pucci, R. Barberi, G. Lombardo, *J. Cataract Refract. Surg.* **2015**, 41, 446.
- [8] G. Lombardo, N. Micali, V. Villari, S. Serrao, M. Lombardo, *Invest Ophthalmol. Vis. Sci.* **2016**, 57, 476.
- [9] S. Baiocchi, C. Mazzotta, D. Cerretani, T. Caporossi, A. Caporossi, *J. Cataract Refract. Surg.* **2009**, 35, 893.
- [10] M. Lombardo, N. Micali, V. Villari, S. Serrao, G. Pucci, R. Barberi, G. Lombardo, *J. Cataract Refract. Surg.* **2015**, 41, 2283.
- [11] G. Brummer, S. Littlechild, S. McCall, Y. Zhang, G. W. Conrad, *Invest Ophthalmol. Vis. Sci.* **2011**, 52, 6363.
- [12] Y. Zhang, A. H. Conrad, G. W. Conrad, *J. Biol. Chem.* **2011**, 286, 13011.
- [13] B. Holmström, G. Oster, *J. Am. Chem. Soc.* **1961**, 83, 1867.
- [14] S. Sel, N. Nass, S. Pötzsch, S. Trau, A. Simm, T. Kalinski, G. I. W. Duncker, F. E. Kruse, G. U. Auffarth, H.-J. Brömme, *Redox Rep.* **2014**, 19, 72.79.
- [15] A. S. McCall, S. Kraft, H. F. Edelhauser, G. W. Kidder, R. R. Lundquist, H. E. Bradshaw, Z. Dedeic, M. J. C. Dionne, E. M. Clement, G. W. Conrad, *Invest Ophthalmol. Vis. Sci.* **2010**, 51, 129.
- [16] P. Kamaev, M. D. Friedman, E. Sherr, D. Muller, *Invest Ophthalmol. Vis. Sci.* **2012**, 53, 2360.
- [17] G. Lombardo, V. Villari, N. Micali, N. Leone, C. Labate, M. P. De Sando, M. Lombardo, *J. Biophotonics* **2018**, 11, e201800028.
- [18] M. Lombardo, G. Lombardo, *J. Cataract Refract. Surg.* **2019**, 45, 80.
- [19] G. Lombardo, S. Serrao, M. Lombardo, *Graefes. Arch. Clin. Exp. Ophthalmol.* **2020**, 258(4), 829.
- [20] X. Ai, J. Mu, B. Xing, *Theranostics* **2016**, 6(13), 2439.
- [21] R. Koprowski, *J. Geophys. Res. Planets* **2014**, 13, 150.
- [22] R. Koprowski, H. Kasprzak, Z. Wrobel, *Comput. Methods Biomech. Biomed Imaging Vis.* **2014**, 5, 27.
- [23] H. Kasprzak, A. Boszczyk, *J. Biophotonics* **2016**, 9(5), 436.
- [24] M. Francis, H. Matalia, R. M. M. A. Nuijts, B. Haex, R. Shetty, A. S. Roy, *J. Refract. Surg.* **2019**, 35(11), 730.
- [25] X. Qin, L. Tian, H. Zhang, X. Chen, L. Li, *J. Geophys. Res. Planets* **2019**, 18, 42.
- [26] Koprowski R. Image Analysis for Ophthalmological Diagnosis in Studies in Computational Intelligence. Springer ISBN: 978-3-319-29546-6, vol. 631, **2016**.
- [27] R. Rushad Shroff, M. Francis, N. Pahuja, L. Veebooy, R. Shetty, A. S. Roy, *Trans. Vis. Sci. Tech.* **2016**, 5(5), 12.
- [28] A. S. Roy, M. Kurian, H. Matalia, R. Shetty, *J. Mech. Behav. Biomed. Mater.* **2015**, 48, 173.
- [29] D. H. Glass, C. J. Roberts, A. S. Litsky, P. A. Weber, *Invest Ophthalmol. Vis. Sci.* **2008**, 49(9), 3919.
- [30] P. Mahendradas, M. Francis, M. R. Vala, P. B. Gowda, A. Kawali, R. Shetty, A. S. Roy, *Ocular Immunol. Inflammation.* **2019**, 27, 1127.
- [31] M. Jannesari, P. Mosaddegh, M. Kadkhodaei, et al., *Mech. Time-Depend. Mater.* **2019**, 23, 373.
- [32] I. Simonini, A. Pandolfi, *J. Mech. Behav. Biomed. Mater.* **2016**, 58, 75.
- [33] J. Matalia, M. Francis, S. Tejwani, G. Dudeja, N. Rajappa, R. A. Sinha, *J. Refract. Surg.* **2016**, 32(7), 486.
- [34] M. Francis, N. Pahuja, R. Shroff, R. Gowda, H. Matalia, R. Shetty, E. J. Remington Nelson, A. S. Roy, *J. Cataract Refract. Surg.* **2017**, 43(10), 1271.
- [35] N. Pahuja, N. R. Kumar, M. Francis, S. Shanbagh, R. Shetty, A. Ghosh, A. S. Roy, *Curr. Eye Res.* **2016**, 41(11), 1419.
- [36] K. M. Metzler, A. M. Mahmoud, J. Liu, C. J. Roberts, *J. Cataract Refract. Surg.* **2014**, 40(6), 888.
- [37] M. Á. Ariza-Gracia, J. F. Zurita, D. P. Piñero, J. F. Rodríguez-Matas, B. Calvo, *PLoS ONE* **2015**, 10(3), e0121486.
- [38] F. Bao, M. Deng, Q. Wang, J. Huang, J. Yang, C. Whitford, B. Geraghty, A. Yu, A. Elsheikh, *Exp. Eye Res.* **2015**, 137, 11.
- [39] B. A. Nguyen, C. J. Roberts, M. A. Reilly, *Front. Bioeng. Biotechnol.* **2019**, 6, 210.
- [40] E. Rosenblatt, P. S. Hersh, *J. Cataract Refract. Surg.* **2016**, 42, 596.
- [41] N. Soeters, N. G. Tahzib, *Optom. Vis. Sci.* **2015**, 92, 329.
- [42] E. Spoerl, F. Raiskup, D. Kampik, G. Geerling, *Curr. Eye Res.* **2010**, 35(11), 1040.
- [43] D. Kampik, B. Ralla, S. Keller, M. Hirschberg, P. Friedl, G. Geerling, *Invest Ophthalmol. Vis. Sci.* **2010**, 51, 3929.
- [44] D. M. Gore, A. Margineanu, P. French, D. O'Brart, C. Dunsby, B. D. Allan, *Invest Ophthalmol. Vis. Sci.* **2014**, 55, 2476.

AUTHOR BIOGRAPHIES

Giuseppe Lombardo is an electronic engineer with PhD in electronics and Master's Degree in biomedical engineering. He is researcher at the Institute for Chemical and Physical Processes of the National Research Council (CNR - IPCF) in Italy. His main scientific interests are devoted to study of optical and mechanical properties of soft matter. He is also keen in numerical modeling and has experience in image processing and pattern recognition algorithms application in biomedical images. He has published more than 100 papers in peer-reviewed journals and is coinventors in nine patents' families.

Giuseppe Massimo Bernava holds a BSc in Computer Engineering and PhD in Computer Science. He is research technologist at the Institute for Chemical

and Physical Processes of the National Research Council (CNR - IPCF) in Italy. He is expert at applications of deep learning in the medical field; Over the years he has been involved in the design and development of multi-platform systems for the realization of intelligent interfaces primarily to define and customize tele-rehabilitation services. He has published more than 20 papers in peer-reviewed journals.

Sebastiano Serrao graduated with honors in Medicine and Surgery and specialized with honors in Ophthalmology, PhD in Refractive Surgery. He is an expert in the field of anterior segment eye surgery, and has strong technical competence in clinical validation of innovative products for eye care. He serves, on a regular basis, as reviewer for more than 10 scientific journals in the field of applied optics, microscopy and vision science. He published more than 70 articles in peer-reviewed scientific journals and co-authored 5 books in the field of ophthalmology.

Marco Lombardo was graduated in Medicine and Surgery in 1999 (summa cum laude) and specialized in Ophthalmology in 2003 (summa cum laude); he earned his PhD in Biomedical Engineering and Computer Science in 2007. He has developed a number of innovative medical devices and ophthalmic formulations for the prevention and treatment of major eye diseases. He published more than 90 papers in peer-reviewed scientific journals and co-authored six books in the field of human optics, corneal biomechanics and corneal surgery. He is co-inventors in three patents' families.

How to cite this article: G. Lombardo, G. M. Bernava, S. Serrao, M. Lombardo, *J. Biophotonics* 2022, 15(12), e202200218. <https://doi.org/10.1002/jbio.202200218>